INTERNATIONAL SOCIETY FOR SOIL MECHANICS AND GEOTECHNICAL ENGINEERING

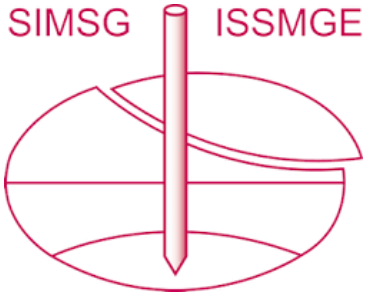

This paper was downloaded from the Online Library of the International Society for Soil Mechanics and Geotechnical Engineering (ISSMGE). The library is available here:

https://www.issmge.org/publications/online-library

This is an open-access database that archives thousands of papers published under the Auspices of the ISSMGE and maintained by the Innovation and Development Committee of ISSMGE.

The paper was published in the proceedings of the 11th Australia New Zealand Conference on Geomechanics and was edited by Prof. Guillermo Narsilio, Prof. Arul Arulrajah and Prof. Jayantha Kodikara. The conference was held in Melbourne, Australia, 15-18 July 2012.

Design Guidelines and Full Scale Verification for MSE Walls with Traffic Barriers Impacted by Vehicles

BRIAUD, J.-L.[1] and SAEZ, D.[2]

[1]Professor, Zachry Department of Civil Engineering, Texas A&M University, College Station, Texas, 77843-3136, USA; Phone: (979)-845-3795; email: briaud@tamu.edu
[2]Graduate Research Assistant, Zachry Department of Civil Engineering, Texas A&M University, College Station, Texas, 77843-3136, USA; Phone: (979)-845-3795; email: dsaez01@neo.tamu.edu

1. ABSTRACT

Current design practices of Mechanically Stabilized Earth (MSE) retaining walls for highway application required the use of an L shaped barrier-foundation systems on top of the wall to contain the impact of an errant vehicle. These design procedures are moving from an Allowable Stress Design (ASD) method to a Load and Resistance Factor Design (LRDF) method. This change includes consideration of new design parameters that has not been properly defined for the LFRD design approach. Therefore, the bases of this paper is to help understand the dynamic behavior of the system under impact loads, to develop a design guideline procedure based on the LRFD design approach and to verify the propose design guideline. In a first part, an analytical and experimental approach used to better understand the behavior of the barrier-moment slab system is described. The results of a static load test and two impact tests on the same full scale barrier are also presented. Guidelines for the dimensions of the barrier-moment slab system are presented and justified on the basis of the work described. In a second part, the results of 4 full scale impact tests against barriers of different shape placed on top of an instrumented MSE wall are presented. The results of these tests were used to develop the design guidelines of MSE wall with traffic barriers impacted by vehicles. In a third part, a full-scale crash test on an instrumented MSE wall is described and analyzed. The wall and barrier behaved satisfactorily and represented a verification of the proposed guidelines. Finally, conclusions are drawn on the basis of the evidence presented and recommendations are made for future approach.

Keywords: retaining walls, traffic barriers, Allowable Stress Design (ASD), Load and Resistance Factor Design (LRFD), barrier-moment slab systems.

2. INTRODUCTION

Pavements are often built on top of MSE walls. The most common case is the case of an MSE wall supporting the access embankment for an overpass. Because cars and trucks travel on top of the MSE wall, traffic barriers are required. In the case of a concrete pavement, these barriers are rigidly tied to the pavement to provide the resistance needed when an impact load is generated by an errant car or truck. In the case of an asphalt pavement, that resistance is not available and the barrier must resist the impact load on its own. In this case an L shaped barrier-moment slab system is used (Briaud et al. 2008) and the resistance is generated by the inertia force required to lift the moment slab (bottom part of the L). The impact load also generates forces in the MSE wall reinforcement and wall panels in addition to the static loads due to gravity.

This paper describes the results of a project sponsored by the National Cooperative Research Highway Program (NCHRP) titled: *"Design of Roadside Barrier Systems Placed on MSE Retaining Walls"*. In the first part, the barrier stability was studied through load testing and numerical simulation and recommendations were made (Briaud et al. 2008 and Bligh et al. 2009). In the second part, a 1.89 m high wall was constructed and instrumented, and the barrier was impacted by a 2,268 kg bogie at approximately 35.41 km/h head on (Bligh et al. 2009 and Kim et al. 2010). The results of these crash tests along with the readings on the instruments and the numerical simulations helped draft preliminary guidelines. The third phase of the project consisted of the proposed guidelines and a full-scale test to evaluate the guidelines. This full-scale test is a pick-up truck crash test on a barrier built atop a 2.79 m high instrumented MSE wall. This section also describes the guidelines including the geotechnical design of the MSE wall to contain the truck impact, then the full-scale crash test with the pick-up truck with the results, and then how the result confirm the guidelines. Note that numerical simulations of the

impact were also carried out to help in finalizing the guidelines presented here and are described elsewhere (Bligh et al. 2009).

3. DESIGN IMPACT LOADS

The design loads for evaluation of barriers placed on top of MSE retaining wall are based on the current design loads presented in AASHTO LRFD Table A13.2-1 “Design Forces for Traffic Railings” (AASHTO LRFD 2007). These design forces correspond to test levels defined in NCHRP Report 350, "*Recommended Procedures for the Safety Performance Evaluation of Highway Features*" (Ross et al. 1993). This report contains six test levels for evaluation of longitudinal barriers. Test levels 1 through 3 (TL-1 to TL-3) refers to passenger vehicles (820C to 2000P) and vary by impact speed and impact angle. Test levels 4 through 6 retain consideration of passenger cars, but also incorporate consideration of heavy trucks. The research presented in this paper covers TL-3(11) impacts, which, according to the definition of NCHRP Report 350, refers to a pick-up truck weighting 2000 kg impacting the barrier at speed of 100 km/hr. at an angle of 25 degrees.

The AASHTO LRFD design loads for TL-3 is 240 kN. This load was derived using data from the instrumented wall testing program conducted at TTI during the 1980’s (Beason and Hirsch 1989). The barrier is evaluated using the ultimate strength design procedure (yield line analyses) described in AASHTO LRFD. However, the AASHTO Manual for Assessing Safety Hardware (MASH) was published in 2009 (MASH 2009). This report is an update to NCHRP Report 350 as an assessment procedure for the performance evaluation of traffic barriers. MASH was developed under NCHRP Project 22-14(2), ‘*Improvement Procedures for Safety-Performance Evaluation of Roadside Feature*” by researchers at Midwest Roadside Safety Facility (MwRSF) at the University of Nebraska. Changes included new design test vehicles, revised test matrices, and revised impact conditions (vehicle mass, impact velocity and impact angle). A comparison between the NCHRP Report 350 and the MASH specification is shown in Table 1.

The new changes introduced by MASH have led to a need of revising the existing design loads recommended in the AASHTO LRFD specification. Under an ongoing research project, sponsored by NCHRP, researchers at the Texas Transportation Institute (TTI) at Texas A&M University conducted an extensive study using existing full-scale crash testing and finite element analyses (FEA) to help update the design loads to be in accordance with MASH. This study has been focused on heavy vehicle impact (TL-4 and TL-5) since the changes incorporated in MASH for passenger cars and pick-up trucks did not substantially increased the design impact load. The preliminary results of this investigation are presented in Table 2.

Table 1: Comparison of test matrices between NCHRP Report 350 and MASH (Ross et al. 1993; MASH 2009)

NCHRP Report 350		*MASH*	
Test Vehicle Designation and Type	Vehicle Weight, kg/ Imp. Velocity, km/h/ Imp. Angle, degrees	Test Vehicle Designation (Vehicle Type)	Vehicle Weight, kg/ Imp. Velocity, km/h/ Imp. Angle, degrees
700C (Small Car)	700/50/20	1100C (Passenger Car)	1100/50/25
820C (Small Car)	820/70/20	1500A (Passenger Car)	1500/70/25
2000C (Pickup Truck)	2000/100/25	2270P (Pickup Truck)	2270/100/25
8000S (Single-Unit Van Truck)	8000/80/15	10000S (Single-Unit Truck)	10000/90/15
36000V (Tractor-Van Trailer)	36000/80/15	36000V (Tractor-Van Trailer)	36000/80/15
36000T (Tractor-Tank Trailer)	36000/80/15	36000T (Tractor-Tank Trailer)	36000/80/15

Table 2: Recommended design loads for TL-4 and TL-5 impact (Bligh et al. 2011)

Design Forces and Designations	TL-3[(a)]	TL-4	TL-5	
Rail Height, H (m)	0.81	≥0.91	1.07	>1.07
F_t Transverse (kN)	240	356	712	1157
F_L Longitudinal (kN)	80	120	334	334
F_v Vertical (kN)	20	169	712	356
Longitudinal Distribution, L_L (m)	1.22	1.22	3.05	3.05
Vertical Distribution, L_v (m)	5.5	5.5	12.2	12.2
Application Point, $H_{e\text{-min}}$ (m) [(b)]	0.6	0.76	0.86	1.1[(c)]

[(a)] As currently defined in AASHTO LRFD
[(b)] Vertical height of the resultant load.
[(c)] If barriers taller than 1.37 m are used, use $H_{e\text{-min}}$= 1.32 m.

4. CURRENT PRACTICE

AASHTO is in the process of changing from Allowable Stress Design (ASD) to Load and Resistance Factor Design (LRFD) (AASHTO LRFD 2007). The 2004 AASHTO ASD makes use of a 44.5 kN equivalent static design load for the design of the traffic barrier and of the MSE wall below (in the form of added load for the reinforcement). The 2007 AASHTO LRFD makes use of a 240 kN design load corresponding to TL-3 for the design of the traffic barrier and a 44.5 kN design load for the design of the MSE wall. Therefore, there has been a significant increase in the design load for the barrier. The increase from 44.5 kN equivalent static load to 240 kN dynamic load for the structural design of the barrier (design criterion 1: breaking the barrier) does not increase the size of the barrier significantly because 44.5 kN is used with an elastic design analysis while 240 kN is used with an ultimate strength analysis. However when it comes to the moment slab design, the change from 44.5 kN equivalent static to 240 kN dynamic requires a proportional increase in the width of the moment slab if the 240 kN is taken as an equivalent static load. This is where the controversy is. Indeed one would calculate a 1.37 m wide moment slab with AASHTO ASD and a 1.37 m x 240/44.5 = 7.4 m wide moment slab with AASHTO LRFD. This comes from the fact that 240 kN is taken as a static load when in fact it is a dynamic load. From experience, practitioners think that a 7.4 m wide moment slab would be unreasonably conservative. The question is to find out how to take into consideration the 240 kN for overturning and sliding of the barrier.

The design of the barrier against overturning consists of applying the load to the barrier at the prescribed height and then using moment equilibrium to find out how wide the moment slab has to be while satisfying a factor of safety against overturning equal to 2. This factor of safety of 2 is consistent with the requirement for overturning of an MSE wall but is not written in the AASHTO ASD for overturning of barriers. The point of rotation for the analysis is taken to be at the bearing point between the barrier and the soil. The design of the barrier against sliding consists of applying the load to the barrier and then using horizontal equilibrium to find out how wide the moment slab has to be while satisfying a factor of safety of 1.5. This factor of safety of 1.5 is consistent with the requirement for sliding of an MSE wall but is not written in the AASHTO ASD for sliding of barriers.

In LRFD, the recommendations are not as detailed. The load factor γ is taken as 1.0 for load combination of Service I and the resistance factor for sliding as 0.8 for cast in place concrete on soil. There are no recommendations for the resistance factor against overturning.

5. STATIC AND DYNAMIC STUDY

A static and dynamic study was conducted on a barrier-moment slab system to help evaluate the kinematic behavior of the system when subjected to a static and dynamic load. The maximum static and dynamic forces resisted by a barrier in a sliding failure mode and in an overturning failure mode were determined and compared to quantify the dynamic amplification factor (DAF). These analyses

were performed by conducting full-scale tests and FEA using the commercially available finite element program LS-DYNA (*LS-DYNA* 2007). Figure 1 shows the section of the barrier-moment slab system used to conduct the static and the dynamic study.

The first part of these studies was to estimate the force required to generate sliding (F_s) and overturning (F_o) of the barrier-moment slab system using equilibrium equations. These forces were computed using eq. (1) for sliding and eq. (2) for overturning:

$$F_s = W \tan\phi \quad (1)$$
$$F_o = W\, l \,/\, h \quad (2)$$

where W is the weight of the barrier- moment slab-soil system (69.6 kN), tanϕ is the moment slab-soil frictional coefficient, ϕ is the friction angle of the soil, *l* is the moment arm of the weight of the system (0.369 m), and *h* is the moment arm of the force applied to the system (1.21 m).

The results of these analyses are shown on Figure 2 as a function of the length of the barrier-moment slab system. For the 3.05 m length barrier system, the required static force is 46.96 kN for sliding and 22.8 kN for overturning. Based on these results, overturning controls the stability of the system.

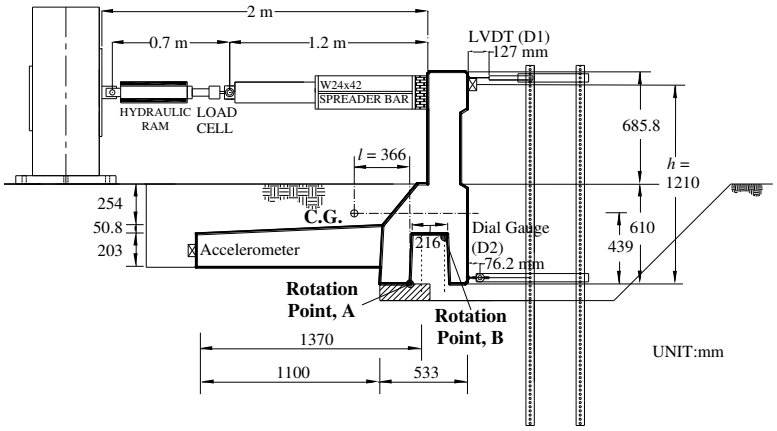

(a)

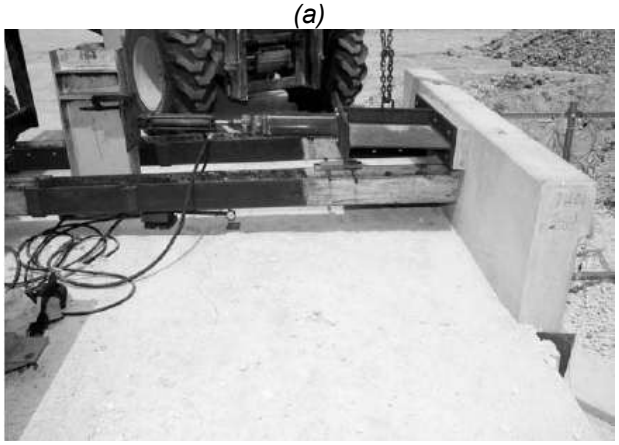

(b)

Figure 1: (a) Details of the barrier-moment slab system and (b) static test. (Briaud et al. 2008)

The second part of these studies was to develop a Finite Element (FE) model of the barrier-moment slab system using LS-DYNA (LS-DYNA 2007). The objectives were to simulate both static and dynamic behavior system. The results of the FEA were used to help plan the full-scale static and dynamic test conducted on the barrier-moment slab system. The vertical parapet, moment slab, and overburden soil were described using solid elements. The vertical parapet and moment slab were rigid materials. The soil was an elastic-plastic soil using a two invariant geologic cap model *(*LS-DYNA 2007*)*. The FEA showed that the system failed by overturning, not by sliding. The result of the simulation for the static test is presented in Figure 3 as a load displacement curve. The maximum load in the simulation is 35 kN while the static hand calculations gives 22.8 kN. The difference is that the

soil resistance at the edges surrounding the moment slab is included in the simulation but not in the hand calculations.

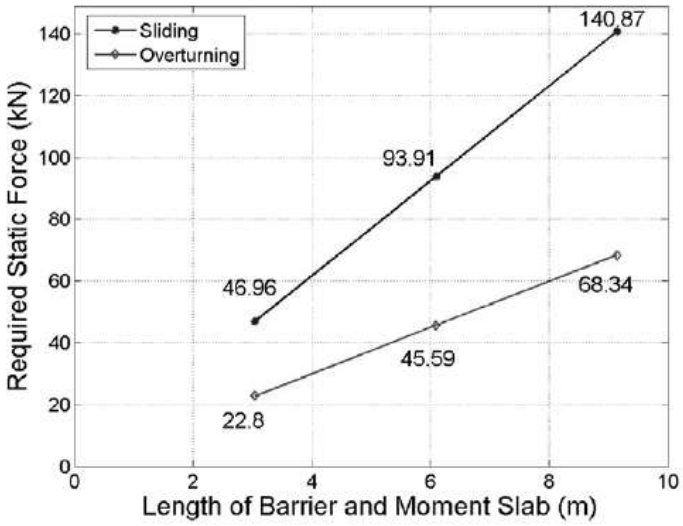

Figure 2: Required Static Force to Induce Sliding or Overturning (Briaud et al. 2008)

The third part of these studies was to conduct a full-scale static and dynamic test. The static load test was conducted prior to the dynamic bogie impact tests. The purpose of the static test was to quantify the magnitude of force required to initiate movement of the barrier-coping-moment slab system. The setup for the static load test of the barrier system is illustrated in Figure 1. The load was measured with a load cell and distributed over a longitudinal barrier length of 1 m through the use of a spreader beam. The load test was stopped at a load of 40 kN. The force-displacement curves generated from the test data are shown in Figure 3. The load-deflection response of the barrier-coping-moment slab system was linear up to a load of 22.3 kN. This load corresponds quite well with the load capacity of this 3 m barrier system based on the rigid body, static equilibrium analysis shown previously (Figure 2).

Figure 3(a) shows the load test results compared to the numerical simulation and the hand calculation. This comparison indicates that the static resistance is made of two components: the component due to the weight of the moment slab and overburden soil, and the component due to the friction between the moment slab-overburden soil and the surrounding soil. Back-calculations indicate that the average shear strength of the concrete soil interface at that shallow depth was 6.3 kPa. The results confirm that overturning is the likely mode of failure since sliding develops more resistance. This comparison also gives credibility to the numerical simulation.

Upon completion of the static load test, the soil on and around the moment slab was recompacted for the dynamic bogie impact. Two head-on impact tests were conducted using a 2,268 kg bogie vehicle, shown in
Figure ***4***. The impact velocity of the first and second bogie impact tests was 21 km/h and 29 km/h, respectively. These velocities were determined using FEA. The targets affixed to the end of the vertical barrier section were used as reference points to determine angular and translational displacement of the barrier from a high-speed video tape. Figure 5 shows the results of the maximum dynamic displacement of the barrier in the horizontal direction from the two dynamic tests. From film analyses, the dynamic displacement of the barrier for the first test was 125 mm at the top (D1) and 69 mm at the ground level (D2). For the second test, the dynamic displacement of the barrier for the first test was 200 mm at the top (D1) and 104 mm at the ground level (D2).

Figure 6 shows the comparison of the load displacement curves for the full-scale static test and the dynamic tests. As can be seen the ratio between peak dynamic force and the peak static force is 4.5 for the 21km/h impact test and 5.4 for the 29 km/h impact test.

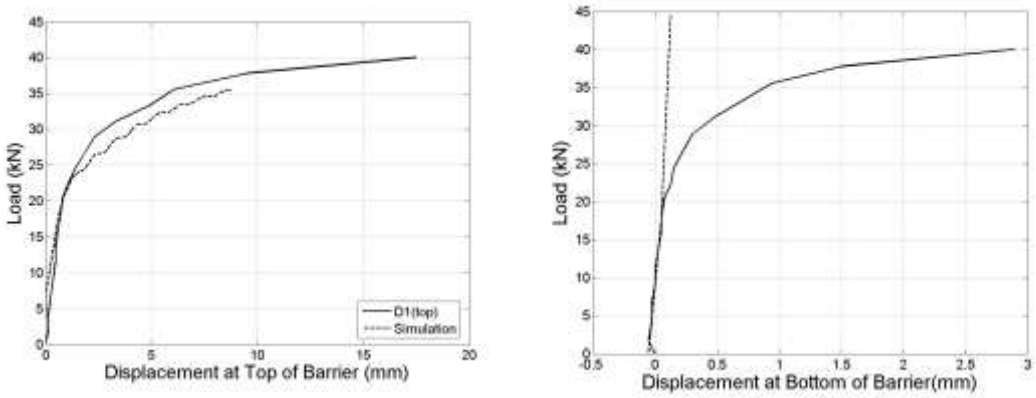

(a) (b)

Figure 3: (a) Comparison of static test and FE static model at D1 and (b) static test at D2. (Briaud et al. 2008)

Figure 4: Bogie test with bogie. (Briaud et al. 2008)

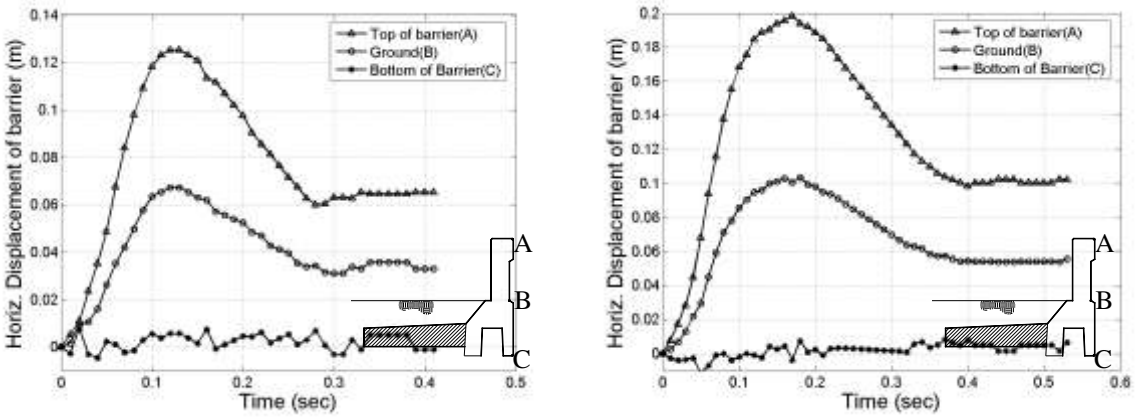

(a) (b)

Figure 5: Horizontal displacement of barrier measured from the film of the (a) 21km/h, and (b) 29 km/h impact test (Briaud et al. 2008)

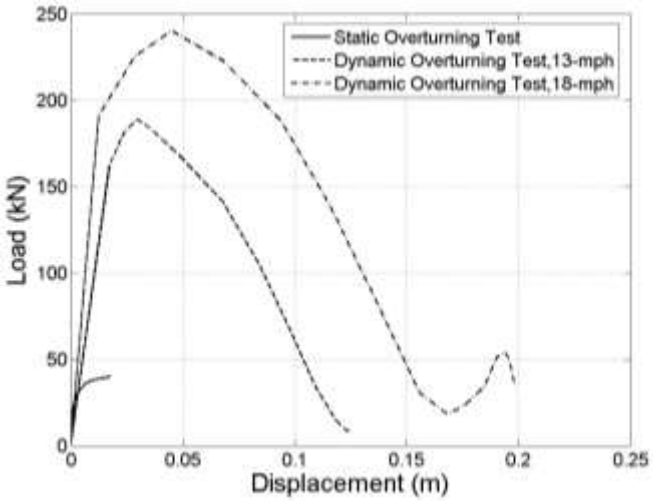

Figure 6: Comparison of static and dynamic overturning tests (Briaud et al. 2008)

6. FULL-SCALE TEST WALL TO DEVELOP THE GUIDELINES

A test wall of 18.3 m long and 1.52 m high was constructed and instrumented. Four impact tests were conducted using a bogie vehicle of 2268 kg. The objectives of the tests were to quantify the movement of the barrier, the moment slab, and the wall panels during impact, and to measure the barrier impact force and the forces in the reinforcement during impact. An elevation of the test installation is shown in Figure 7.

6.1 Design, construction and instrumentation of the test wall

The test wall was designed based on the Load and Resistance Factor Design (LRFD) procedure outlined in the AASHTO Standard Specifications for Highway Bridges (AASHTO 2004). The expected forces on the soil reinforcement due to the design impact load were calculated and compared to those measured in the dynamic impact experiments.

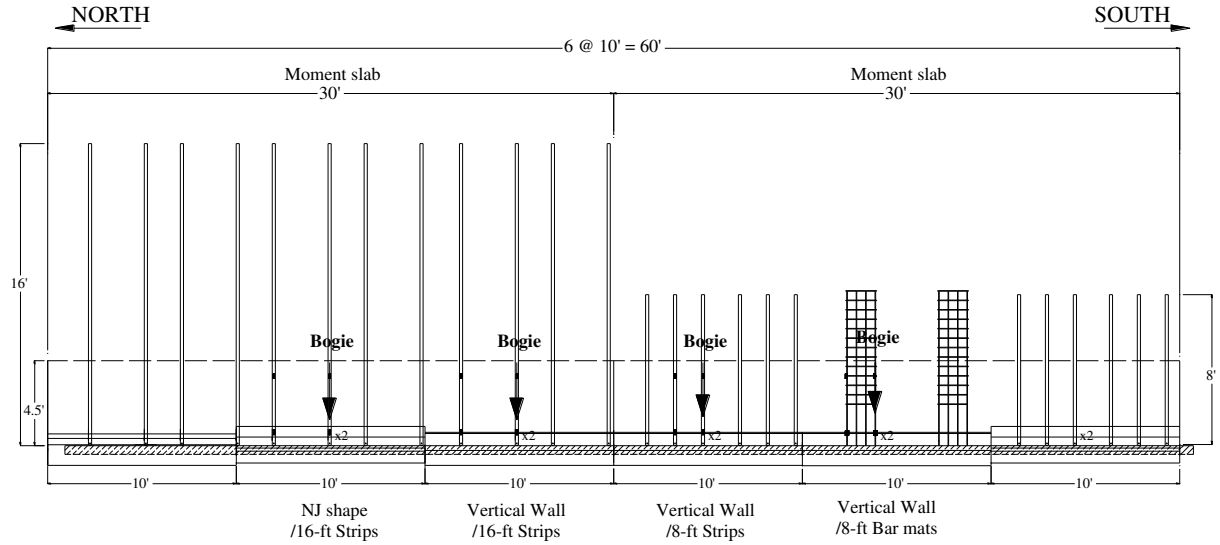

(a) Plan view of test plan.

Figure 7: *Instrumented test wall (Kim et al. 2010)*

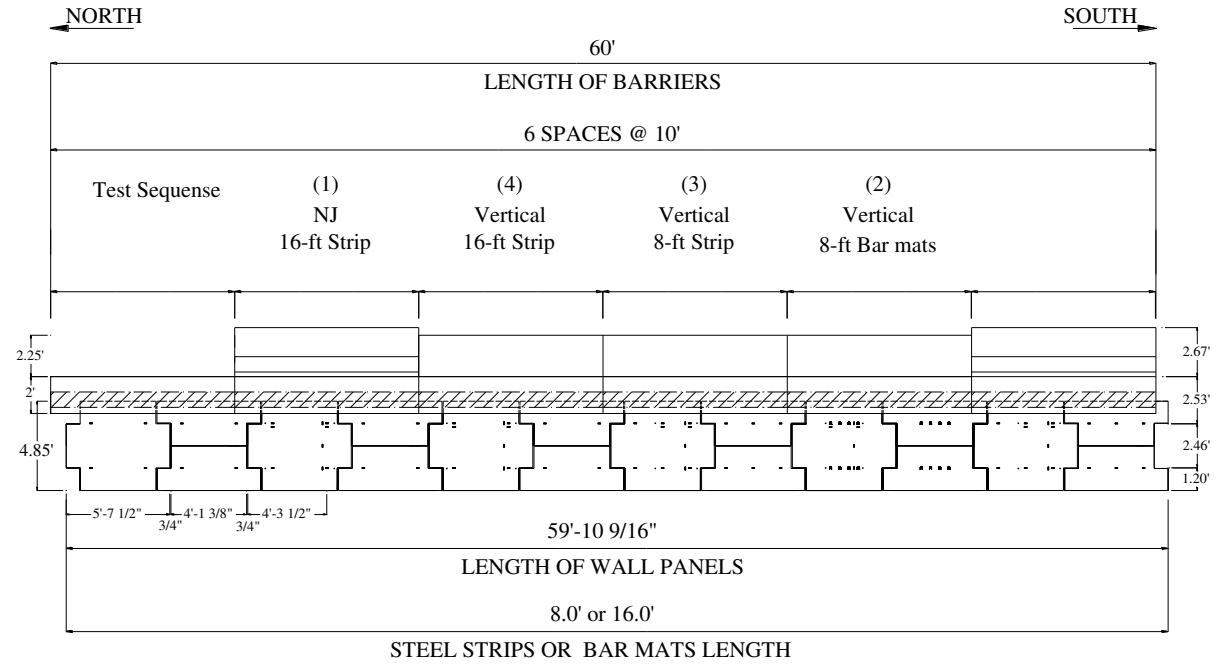

(b) Elevation view of test plan.

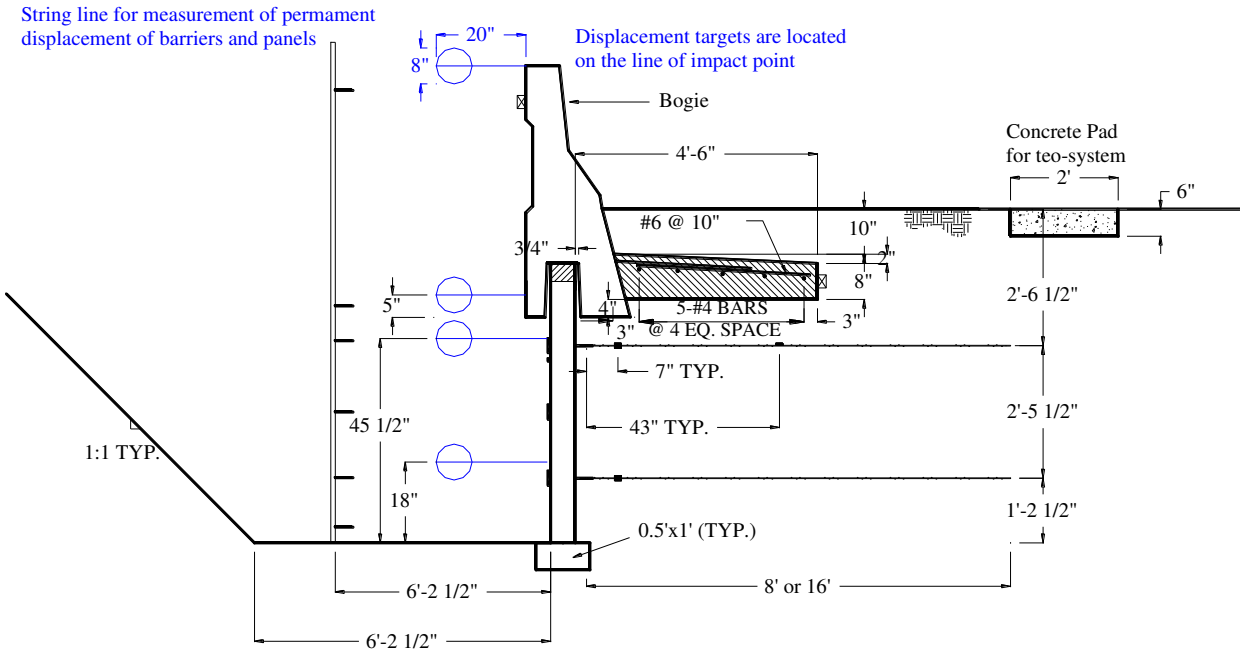

(c) Side view of test plan (test 1)

Figure 7 : Instrumented test wall (continued) (Kim et al. 2010)

To calculate the force T expected in each strip due to the soil weight and the impact load, the following equation in AASHTO-LRFD was used:

$$T = A_t \times \left(\sigma_h + \Delta\sigma_{h,\max} \right) \tag{3}$$

where A_t is the panel tributary area of one strip, σ_h is horizontal stress due to the soil weight ($\sigma_h = K_r \times \sigma_v$), K_r is the horizontal earth pressure coefficient given by 1.7 K_a, $\Delta\sigma_{h,max} = 2P_{hl} / l_1$ is the horizontal stress due to the impact load P_{h1} on the barrier, and l_1 is the depth of influence of the impact load down the wall face.

To calculate the factored pullout resistance of the soil reinforcement the following equation in AASHTO-LRFD was used:

$$P = F^{*} \times \alpha \times \sigma_{v} \times C \times L_{e} \quad (4)$$

where P is the ultimate pullout resistance (AASHTO LRFD Eq. 11.10.6.3.2-1), F^{*} is the pullout friction factor (AASHTO LRFD Figure 11.10.6.3.2-1), α is the scale effect correction factor (AASHTO LRFD Table 11.10.6.3.2-1), σ_v is the vertical stress at the depth of the soil reinforcement, C is the overall reinforcement surface area geometry factor based on the gross perimeter of the reinforcement and is equal to 2 for strip, grid and sheet-type reinforcements, and L_e is the length of reinforcement in the resisting zone (effective length). Table 3 shows the results of the estimated design load and the calculated factored pullout resistance based on AASHTO-LRFD design procedure.

Table 3: Calculated design and ultimate resistant load in the soil reinforcement

	Test 1 (New Jersey) (4.88 m Long strips) (4 per panel)	Test 2 (Vertical Wall) (2.44 m Long Bar mat) (Ave. load per bar)	Test 3 (Vertical Wall) (2.44 m Long strips) (6 per panel)	Test 4 (Vertical Wall) (4.88 m Long strips) (4 per panel)
Total Design Tensile Load (kN)	6.5 (upper) 8.9 (lower)	4.3 (upper) 6.1 (lower)	4.3 (upper) 6.1 (lower)	6.5 (upper) 8.9 (lower)
AASHTO Pullout Resistance (kN)	13.4 (upper) 23.6 (lower)	6.2 (upper) 11.1 (lower)	6.7 (upper) 12 (lower)	13.4 (upper) 23.6 (lower)

The MSE test wall shown in Figure 7 was 18.29 m long and 1.52 m high (one panel height).The wall-barrier system was planned on the premise that multiple impacts could be conducted on barrier segments connected to the same moment slab. Half of the wall was constructed using two types of 2.44 m long reinforcement (strips and bar mats) while the other half was constructed with 4.88 m long reinforcement strips, as presented in Table 3. The strips were 50 mm wide and 5 mm thick. Each layer of bar mats consisted of two sections of 6 × 6 - W 10 × W 10 bar attached to the wall panel using clevis loops. The 2.44 m long reinforcement represents the minimum length allowed in current practice. Such lengths are commonly used in low height wall segments such as at the beginning or ending of an elevated overpass structure.

The backfill for the wall was crushed rock that met TxDOT specification Type B backfill (TXDOT 2004). The estimated friction angle for the crushed rock was 35 degrees and the unit weight was 20 kN/m^3. The backfill was compacted in 0.15 m layers with 10 passes of a 1320 kg and 0.89 m width drum roller. Also, the surface layer of soil was re-compacted after each test. The panels of the wall were arranged in a succession of one 1.52 m high full panel followed by two 0.76 m high half-panels. All panels were 1.52 m wide. The wall panels were placed on a 0.31 m wide × 0.15 m thick concrete leveling pad.

Six precast barrier and coping sections were placed on top of the wall panels. The panels were recessed inside the coping sections a distance of 0.23 m comprised of 0.1 m of leveling concrete pad plus 0.13 m of engaged panel. The moment slab connecting the precast barrier-coping sections was cast in two 9.15 m lengths connected to one another using two 0.91 m long No. 9 shear dowels. The moment slabs were 1.37 m wide from the back face of the wall panel to the end of the moment slab. The reinforcement was instrumented with strain gages to capture the tensile forces transmitted into the reinforcement during each bogie vehicle impact. A total of 8 strain gages were used for each test. The placement of these strain gages was selected to measure the maximum tensile load in each layer of reinforcement as well as give an indication of the distribution of forces in lateral, longitudinal, and vertical directions. Five strain gages were used on the upper reinforcement layer, and three strain gages were placed on the lower reinforcement layer. Two strain gages were used on both layers of reinforcement adjacent to the wall panel at the point of impact to provide some redundancy at the location expected to experience maximum tensile loading.

A contact switch was placed on the inside face (traffic side) of the concrete leveling pad cast on top of the wall panels to indicate the time at which the barrier came in contact with the wall panel. The wall panel below the point of impact on each barrier was instrumented with five concrete strain gages to

capture normal strains in the panel at impact. Two of the five strain gages were placed in a horizontal direction just below the anchor point of the upper layer of reinforcement (region of maximum negative moment). The other three strain gages were placed in the vertical direction: two were adjacent to the anchorage locations for the upper and lower layer of reinforcement at the point of impact, and one was placed between in the middle of the panel between the two layers of reinforcement (region of maximum positive moment).

An accelerometer was mounted behind each barrier section at the height of impact to help analyze its dynamic response. Another accelerometer was placed at the end of each of the two 9.14 m long moment slabs at their midpoints to measure any acceleration imparted to the moment slab during impact. Additionally, the bogie vehicle was instrumented with an accelerometer.

Rotation as well as vertical and horizontal displacements of the barrier and wall panels were determined from high-speed video operating at 1000 frames/second. Displacement gages were placed at the top and bottom of the precast barrier-coping section and at the upper and lower strip locations on the wall panel to assist with the displacement analysis. Independently secured string lines were placed 1.22 m behind the barrier and wall to measure the permanent deflection of the barrier and wall after impact. The permanent movement of the four corners of the back of the barrier and the permanent movement of five points on each panel were measured after each test.

The test sequence was selected such that the first two tests involved impacting the barrier segments in the middle of each moment slab (one N.J. barrier and one vertical wall). The other two tests were conducted on vertical concrete barrier located at the end of each moment slab with different strip length and density. A 2268 kg bogie vehicle impacted each test section at a speed of approximately 35.4 km/h for the N.J. barrier and 32.19 km/h for the vertical concrete barriers. Loading each barrier near the ultimate load of the barrier ensured that the maximum impact load was transferred into the MSE wall.

6.2 Impact Test Results

Each time the 2268 kg bogie vehicle, shown in Figure 8(b), impacted the barrier head-on at a speed ranging from 32.5 km/h to 35 km/h (the results are summarized in (Table 4). The impact point for each test is shown on Figure 7. The impact point was positioned above the reinforcement that was instrumented to record the maximum impact forces. The test results include accelerometer data and associated forces and displacements (bogie, barrier, moment slab), high speed film analysis, string line measurements and associated displacements (barrier, wall panel), strain gages and associated forces in the reinforcement (strips, bar mats), and accumulated damage of the barrier, soil, and wall panels.

5.2.1 Dynamic impact load and displacement results

Data obtained from the bogie-mounted accelerometer were analyzed and a 50 millisecond (msec.) moving average was generated. The peak accelerations are shown in Table 4. Based on the acceleration and the mass of the bogie, the maximum impact force was calculated as shown in Table 4. Note that the peak impact forces vary from 286.55 kN to 324.72 kN and are all higher than the 240 kN dynamic force associated with the design of barriers for test level 3.

Targets were affixed to the top of the barrier, the bottom of the barrier, and the wall panel at a location corresponding to the top and the bottom layers of reinforcement (Figure 7). The maximum dynamic horizontal displacement at the top of the barrier varied from 131 mm to 156 mm. The maximum dynamic horizontal displacement at the bottom of the barrier varied from 18 mm to 30 mm. The maximum dynamic horizontal displacement of the panel at the top layer of reinforcement varied from 8 mm to 23 mm. The maximum dynamic horizontal displacement of the panel at the bottom layer of reinforcement varied from 0 mm to 5 mm.

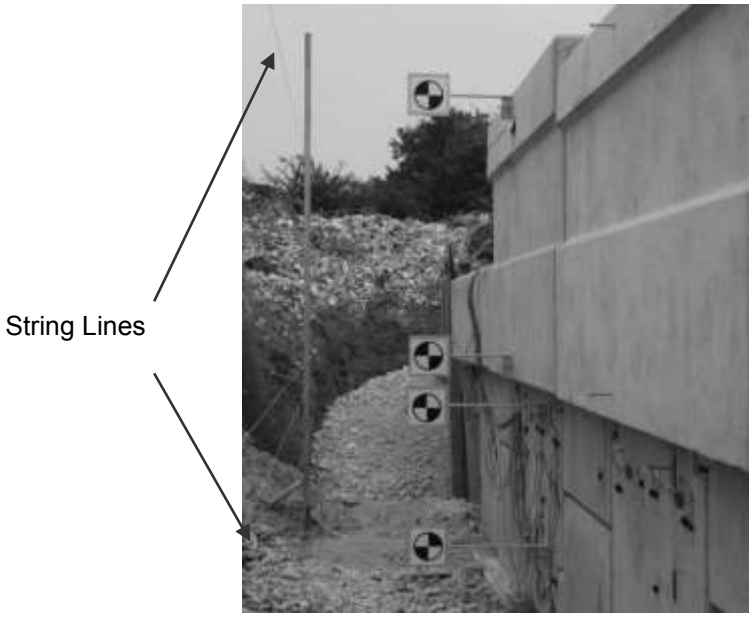

(a) Location of displacement targets and sting line.

Figure 8: MSE wall installation before and after tests (Kim et al. 2010)

(b) Test installation after test.

Figure 8: MSE wall installation before and after tests (continued) (Kim et al. 2010)

The permanent movements of the target locations were obtained in two ways: high speed film analysis and distances from the reference string line stretched in front of the wall (Figure 7). The string line permanent measurements consisted of measuring the distance with a tape measure from the target to the string before and after each test. The permanent horizontal displacement at the top of the barrier varied from 6.3 mm to 99 mm. The permanent horizontal displacement at the bottom of the barrier varied from 8 mm to 20 mm. The permanent horizontal displacement of the panel at the level of the top row of reinforcement varied from 1 mm to 16 mm. The permanent horizontal displacement of the panel at the level of the bottom row of reinforcement varied from 0 mm to 4.1 mm.

Even though the wall systems were subjected to higher loads than design conditions, all movements were considered acceptable from a performance point of view. The wall system comprised of the 2.44 m strip reinforcement (Test 3) lead to the highest panel movements, while the lowest movements were recorded for the configuration that incorporated 4.88 m strips and the vertical wall parapet (Test 4). However, the Test 4 configuration also had the most extensive panel damage. In this test, the top panel exhibited a horizontal flexure crack along a line corresponding to the location of the top layer of reinforcement.

Table 4: Test Matrix and Results (Kim et al. 2010)

	Test 1	Test 2	Test 3	Test 4
Barrier Type	New Jersey	Vertical Wall	Vertical Wall	Vertical Wall
Reinforcement	4.88 m long Strip (4 per panel)	2.44 m long Bar Mat	2.44 m long Strip (6 per panel)	4.88 m long Strip (4 per panel)
Speed of Bogie Vehicle	35.08 km/h	32.67 km/h	32.49 km/h	32.49 km/h
Peak Bogie Acceleration	14.45 g	13 g	13.82g	12.69 g
Impact Force	326.5 kN	294 kN	312.1 kN	286.55 kN
Peak Barrier Acceleration	7.36 g	10.71 g	10.16 g	13.04 g
Peak Moment Slab Acceleration	1.84 g	-	1 g	-
Displacement Top of Barrier (mm)	156 (dynamic) 76.2 (permanent)	153.4 (dynamic) 101.6 (permanent)	131.3 (dynamic) 63.5 (permanent)	152.9 (dynamic) 76.2 (permanent)
Displacement Bottom of Coping (mm)	28.5 (dynamic) 14 (permanent)	24 (dynamic) 12.7 (permanent)	29.5 (dynamic) 15.2 (permanent)	17.5 (dynamic) 5.6 (permanent)
Displacement of Panel (mm) (upper layer)	16 (dynamic) 6.1 (permanent)	9.4 (dynamic) 5.1 (permanent)	23.4 (dynamic) 14 (permanent)	7.6 (dynamic) 1.8 (permanent)
Displacement of Panel (mm) (bottom layer)	No movement	2.5 (dynamic) 0.5 (permanent)	4.8 (dynamic) 4.6 (permanent)	1.8 (dynamic) 0.0 (permanent)
Max, 50 msec Avg. Loads In Strips At Top Layer	31.98 kN* (35.36 kN-T, 28.6 kN-B) **	6.85 kN* (6.41 kN-T, 7.25 kN-B) **	9.47 kN* (-1.33 kN-T, 20.28 kN-B) **	33.18 kN* (33.49 kN-T, 32.92 kN-B) **
Estimated Design Load At Top Layer	23.53 kN	5.03 KN	1.98 kN	24.42 kN
Max, 50 msec Avg. Loads In Strips At Bottom Layer	-5.34 kN* (-2.14 kN-T, -8.54 kN-B) **	0.36 kN* (-0.71 kN-T, 1.38 kN-B) **	5.29 kN* (4.36 kN-T, 6.23 kN-B) **	0.67 kN* (-10.85 kN-T, 12.19 kN-B) **
Estimated Design Load At Bottom Layer	-3.91 kN	0.27 kN	3.91 kN	0.49 kN

6.2.2 Load on the wall reinforcement

The wall reinforcement was instrumented with a total of 32 strain gages (8 for each test) to capture the tensile forces transmitted to the reinforcement during the bogie impacts. The 8 strain gages were placed on 6 strips in two locations: 0.18 m and 1.09 m behind the connection to the panel. Two strips receiving a pair of gages (top and bottom) and the other 4 strips received only one strain gage (top only). Because a fair amount of bending unexpectedly took place in the strips during the impact, the positions which had only one gage did not lead to reliable data. The positions which had two gages permitted cancellation of the bending stresses so that the true tensile load in the strip could be obtained. As a result there are only two strip loads reported for each test in
Figure ***9***. For the bar mats, the strain gages were placed on the bars in similar fashion. The load vs. time history in the reinforcement is a 50 msec. average. Note that the strain gages were zeroed after

the MSE wall was built and, therefore, the loads shown do not include the static load necessary to retain the soil mass.
The maximum dynamic load in the strips (50 msec. average) varied from 6.85 kN (Test 2) to 33.18 kN (Test 4). The higher loads were associated with the 4.88 m long strips while the lower loads were associated with the 2.44 m long reinforcement.

The back-calculated f* values (friction coefficient between the strips and the soil) ranged from 2.58 to 4.51. These measured instantaneous values are much higher than the design recommendation for this case which is 1.79. This is not unusual since the recommended values represent a lower bound of the values measured by many researchers. Note that these friction values are much higher than might seem appropriate at first glance. The reason they are higher than unity is that the strips have ribs which engage the bearing capacity of the surrounding soil in addition to the friction. So, the pull out of strips is not a pure friction phenomenon. The bearing capacity effect is also lumped into the recommended friction factor. Note also that the sum of the strip forces does not have to add to the impact force because other forces contribute to the resistance including the barrier inertia force and the barrier-soil friction force.

A tape switch was adhered to the back face of the leveling pad extension on top of the wall panels. The idea was to identify whether or not the barrier coping contact and engage the panel during an impact event. The contact duration is indicated in
Figure ***9*** by an arrow labeled “tape switch.” Note that sometimes there are two time periods over which the contact took place indicating that a bouncing phenomenon developed.

As previously noted, the peak dynamic loads against the barriers were higher than 240 kN which is the design load prescribed by AASHTO. To obtain the load on the strips for an impact force equal to 240 kN, the loads were reduced by the ratio between the peak dynamic load actually measured and the 240 kN load. So, for Test 1 for example, the strip load corresponding to a 240 kN barrier impact load would be obtained as follows:

Estimated strip load for 240 kN:

$$= \frac{240}{326.6} \times \text{Maximum Measured Strip Load} \quad (5)$$

The estimated strip loads associated with a 240 kN design impact load are shown in Table 4. Note that the peak dynamic impact load on the barrier (*Figure 9*) occurred before the maximum load in the strips. This seems to indicate that there is a lag time between the barrier movement and the soil deformation which engages the strip loads.

The second row of reinforcement experienced much lower loads including compression loads in some cases. The reason for this is attributed to rotation of the panel around the first anchor point provided by the top row of reinforcement. This rotation creates a possible inward movement of the bottom of the panel. This compression can be resisted by a combination of strip load and by pressure against the soil mass.

6.2.3 Damage to the barrier and the panels

In all tests, the most severe damage occurred in the barriers. In a real situation, these barriers would have to be replaced. However, it should be noted that the impact load was designed to fail the barrier and exceeded the 240 kN design load. The N.J. barrier in Test 1 failed along a horizontal line located at the change in thickness of the cross section with some evidence of V-shaped cracks. The vertical wall barrier in Test 2 failed along a combination of half V half horizontal line; the reason is that the point of impact was closer to one edge of the 3.05 m long barrier to position the point of impact over one of the bar mats. The vertical wall barrier in Test 3 failed in a V shape pattern with a horizontal line at its base and so did the vertical wall barrier in Test 4. None of the barriers failed in the assumed V shape associated with a traditional yield line failure but rather in a V shape combined with a horizontal flexure mode.

The damage to the MSE wall panels consisted of spalling around the connection between the top of the panel and the bottom of the barrier. This is attributed to the shearing process that broke the bond

between concrete leveling pad and the wall panels. This spalling took place in all four tests. In addition, in Test 4 (vertical wall with 4.88 m long strips), a flexural crack developed horizontally across the wall panel at the level of the first row of reinforcement.

There was no external evidence of failure of the moment slab, front face of the coping and wall reinforcement. The high speed films did indicate that the edge of the moment slab lifted during impact. A small gap could be seen after the tests at the interface between the moment slab and the soil behind it. Furthermore for the tests near the connection between the two 9.14 m long moment slabs (Tests 3 and 4), the film showed that the edge of the moment slab lifted over the entire 18.29 m indicating that the dowels engaged both 9.14 m length lengths.

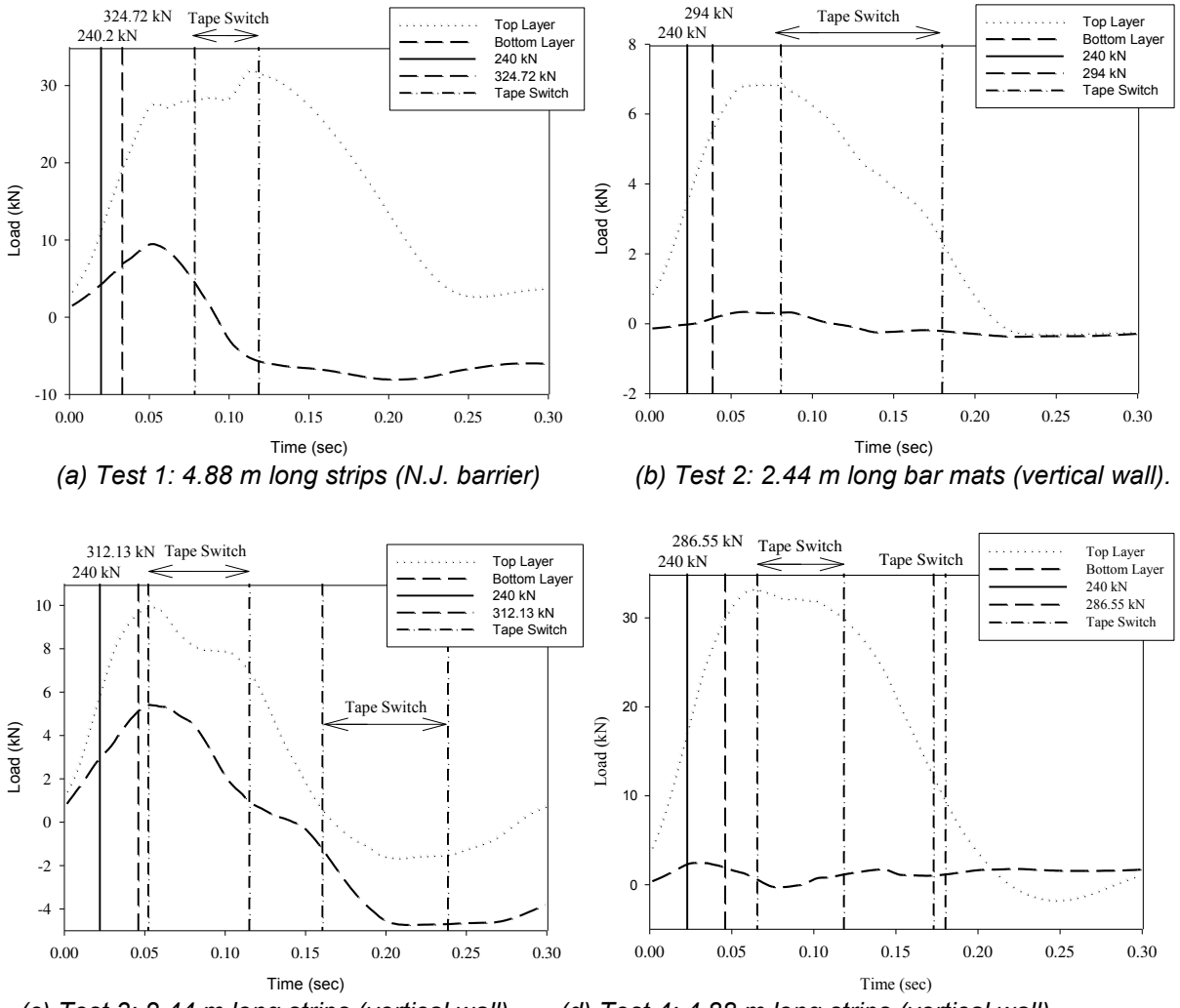

(a) Test 1: 4.88 m long strips (N.J. barrier) *(b) Test 2: 2.44 m long bar mats (vertical wall).*

(c) Test 3: 2.44 m long strips (vertical wall) *(d) Test 4: 4.88 m long strips (vertical wall)*

Figure 9: 50 msec. average load of on the reinforcement (Kim et al. 2010).

7. RECOMMENDED DESIGN GUIDELINES

These guidelines include the barrier-moment slab stability and the geotechnical design of the MSE wall. While the barrier-moment slab stability is not a geotechnical problem it is included here for the sake of completeness and because it helps to understand the geotechnical design of the wall (Kim et al. 2012).

7.1 Stability of the barrier-moment slab system

The guideline for evaluation of stability of the barrier-moment slab system is based on the sliding and the overturning failure mode. For the system to be stable against sliding, the factored static resistance

(ϕP) to sliding along its base must be greater than or equal to the factored equivalent static load (γL_s) due to the dynamic impact force (Figure 10).

$$\phi P \geq \gamma L_s \quad (6)$$
$$P = W \tan \varphi_r \quad (7)$$

where ϕP is the factored static resistance of the system, L_s is the equivalent static load (for load level TL-3, L_s is 44.5 kN according to the results of the aforementioned static and dynamic test), W is the weight of the monolithic section of barrier and moment slab plus any material laying on top of the moment slab and φ_r is the friction angle of the soil-moment slab interface.. The value of ϕ, the resistance factor, is equal to 0.8, and the value of γ, the load factor, is equal to 1.0 because this event is considered to be an extreme event. If the soil-moment slab interface is rough (cast in place), φ_r is equal to the friction angle of the soil φ_s. If the soil - moment slab interface is smooth (precast), φ_r would be reduced accordingly (ϕ_r=2/3tanϕ_s). (Kim et al. 2012).

If the barrier-moment slab system rotates during the impact, the point of rotation influences the response. Depending on the design, two points of rotation of the barrier-moment slab system are possible as shown in Figure 10. The point of rotation is determined based on the interaction between the barrier coping and the top of the wall panel. With reference to Figure 10, the point of rotation is taken as Point A if the top of the wall panel is isolated from contact with the coping by presence of an air gap or sufficiently compressible material. The point of rotation is taken as Point B if there is direct bearing between the bottom of the coping and the top of the wall panel or level up concrete. In the full-scale crash test, the point of rotation was Point B.

For the system to be stable against rotation, the factored static moment resistance (ϕ M) to overturning must be greater than or equal to the factored static load (γ L_s) due to the impact force times the moment arm h_A or h_B taken as the vertical distance from the point of impact due to the dynamic force to the point of rotation A or B (Figure 10).

$$\phi M \geq \gamma L_s (h_A \text{ or } h_B) \quad (8)$$
$$M = W (l_A \text{ or } l_B) \quad (9)$$

where ϕ M is the factored static moment resistance (for load level TL-3, L_s is 44.5 kN as mentioned previously, ϕ is the resistance factor equal to 0.9 and γ is the load factor equal to 1.0), W is the weight of the monolithic section of barrier and moment slab plus any material laying on top of the moment slab, and l_A or l_B is the horizontal distance from the center of gravity of the weight W to the point of rotation A or B. The moment contribution due to any coupling between adjacent moment slabs, shear strength of the overburden soil, or friction which may exist between the backside of the moment slab and the surrounding soil is neglected (Kim et al. 2012).

During the impact, the section of the barrier which is most likely the critical section is the narrow part of the coping (Figure 10). This section must be designed to resist the applicable impact load conditions for the appropriate test level as defined in AASHTO LRFD.

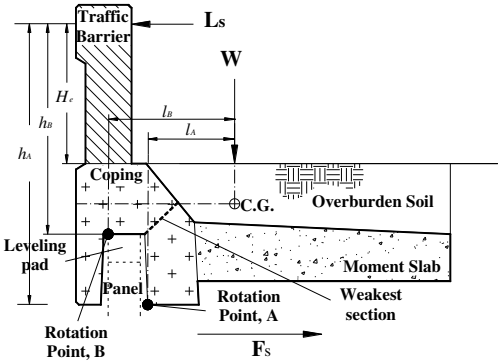

Figure 10: Barrier-moment slab system for barrier design guideline (Kim et al. 2012)

6.2 Pullout of the wall reinforcement

The factored static resistance (ϕ P) to pullout of the reinforcement must be greater than or equal to the sum of the factored static load (γ_s F_s) due to the earth pressure and the factored dynamic load (γ_d F_d) due to the impact. The static load F_s is obtained from the static earth pressure p_s times the tributary area A_t of the reinforcement unit. The dynamic load F_d is obtained either from a pressure distribution p_d (Figure 11(a) for load level TL-3) times the tributary area A_t of the reinforcement unit or the line load Q_d (Figure 11(b) for load level TL-3) times the longitudinal spacing (S_L) of the reinforcement. The two approaches are equivalent and are presented for convenience as some prefer to use pressures and others prefer to use line loads. The pressure distribution and the line loads are based on measurements made during the impact tests in the instrumented test wall presented before (kim et al. 2012).

$$\phi P \geq \gamma_s F_s + \gamma_d F_d \quad (10)$$

$$\phi P \geq \gamma_s p_s A_t + \gamma_d p_d A_t \quad (11)$$

$$\phi P \geq \gamma_s p_s A_t + \gamma_d Q_d S_L \quad (12)$$

where ϕ is the resistance factor equal to 1.0, γ_s is the static load factor equal to 1.0, and γ_d is the dynamic load factor equal to 1.0. The reinforcement resistance P for strips and bar mats is calculated according to AASHTO LRFD guidelines (eq. (4)). Note that eq. (11) with load and resistance factors equal to 1, as recommended, means that the strips can be designed to be at pull out failure during the impact. This is permitted as the pull out failure condition only exists for a very short time (milliseconds) and did not lead to excessive deflections in the experiments (Kim et al. 2012).

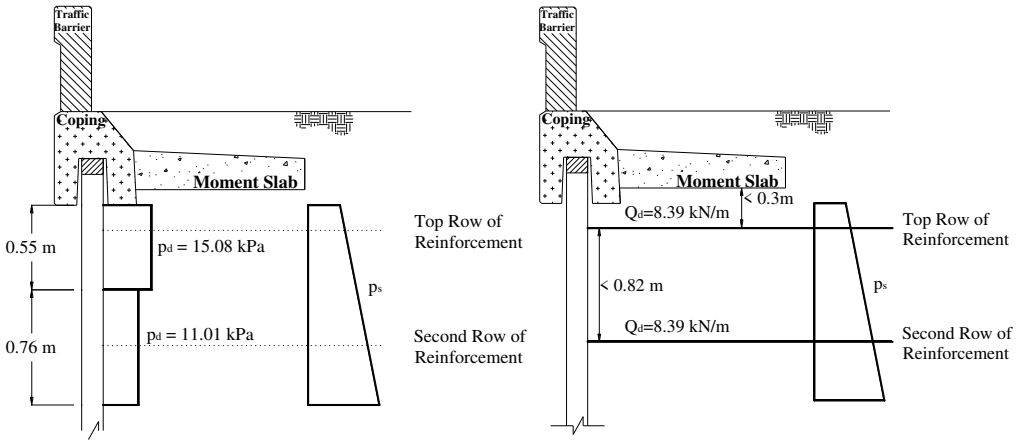

Figure 11: Design load for reinforcement pullout: (a) Pressure distribution p_d, (b) Line load Q_d (Kim et al. 2012).

6.3 Yielding of the wall reinforcement

The factored resistance (ϕ R) to yielding of the reinforcement must be greater than or equal to the sum of factored static load (γ_s F_s) due to the earth pressure and the factored dynamic load (γ_d F_d) due to the impact. The static load F_s is obtained from the static earth pressure p_s times the tributary area A_t of the reinforcement unit. The dynamic load F_d is obtained either from the pressure distribution p_d (Figure 12(a) for load level TL-3) times the tributary area A_t of the reinforcement unit or line load Q_d (Figure 12(b) for load level TL-3) times the longitudinal spacing (S_L) of the reinforcement. The two approaches are equivalent and are presented for convenience as some prefer to use pressures and others prefer to use line loads. The pressure distribution and the line loads are based on measurements made during the impact tests in the instrumented test wall presented before (Kim et al. 2012).

$$\phi R \geq \gamma_s F_s + \gamma_d F_d \quad (13)$$

$$\phi R \geq \gamma_s p_s A_t + \gamma_d p_d A_t \quad (14)$$

$$\phi R \geq \gamma_s p_s A_t + \gamma_d Q_d S_L \quad (15)$$

where ϕ is the resistance factor equal to 1.0, γ_s is the static load factor equal to 1.0, and γ_d is the dynamic load factor equal to 1.0. The reinforcement resistance R for strips and bar mats is calculated by AASHTO LRFD guidelines. Note that eq. (14) with load and resistance factors equal to 1, as recommended, means that the strips can be designed to be at yielding during the impact. This is permitted as the yielding condition would only exist for a very short time (milliseconds) (Kim et al. 2012).

Note that Figure 11 and Figure 12 are different for the following reason. Figure 12 corresponds to the dynamic loads Q_m actually measured in the strips during impact. The strips do experience the load Q_m and must be safe against yielding under these conditions. The loads Q_m measured in the strips were about 4 times higher than the maximum pull out resistance Q_c of the strips calculated according to AASHTO LRFD. Therefore it was decided that the recommended design values for pull out (Figure 11) should be 4 times less than the recommended design values for yielding (Figure 12). This comment applies to the first row of strips but not the second one. For the second row of strips, the measured loads Q_m were not larger than the calculated loads Q_c, therefore the recommended values for the second layer of reinforcement is the same for pull out and yielding (Kim et al. 2012).

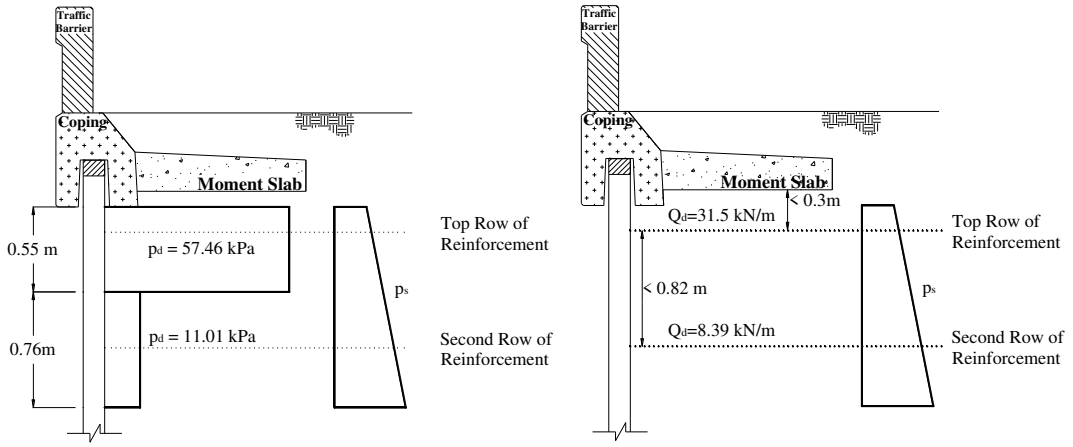

Figure 12: Design load for reinforcement rupture: (a) Pressure distribution p_d, (b) Line load Q_d (Kim et al. 2012).

8. FULL-SCALE CRASH TEST TO VERIFY THE GUIDELINES

7.1 MSE Wall Design, Construction, and Instrumentation

The MSE wall and the barrier-moment slab system were designed according to the above guidelines. An overall layout of the MSE wall that was used for the full-scale crash test verification is shown in Figure 13. The instrumented MSE wall was 27.53 m long and 2.79 m high and the panels were 1.52 m by 1.52 m. The MSE wall had three layers of reinforcement. The steel reinforcement strips were 3.05 m long and the reinforcement had a density of three strips per layer per panel. The barrier-coping sections rested on a 67 mm thick layer of a level-up concrete placed on top of the wall panels. The moment slabs connecting the 3.05 m long precast barrier-coping sections were cast-in-place in three 9.17 m lengths. Three 1.37 m wide × 9.17 m long moment slabs were connected to one another using two 0.9 m long No.9 shear dowels across each joint. To enable comparison of forces and displacements, barriers were assigned alphanumeric designators as shown in Figure 13(a).

The barrier portion of the precast barrier-coping sections consisted of a vertical concrete barrier that conforms to the Texas Type T221 traffic rail. Figure 13(b) shows a cross section of the barrier-coping section and MSE wall.

The MSE wall backfill was made of two layers: poorly graded clean sand from the bottom of the wall to the bottom of the moment slab (2.18 m) and a limestone rock fill usually used as road base from the bottom of the moment slab to the riding surface (0.61 m). Both the sand and the road base layers were properly compacted.

Seven reinforcement strips in the MSE wall were instrumented with strain gages to capture the tensile forces experienced by the reinforcement during the full-scale crash test as shown in Figure 13(a). These strips were selected because numerical simulation results had indicated that they developed the maximum tensile loads during impact. Two strain gages were used at each selected location (one on the top of the strip and one on the bottom of the strip) to compensate for any bending in the strip.
A contact switch was placed on the top edge of the traffic face (inside face) of the wall panels inside the coping recess. The switch was installed to indicate the time of contact in case the barrier would move sufficiently for the coping to contact the wall panel (Figure 13 (b)).

Two accelerometers were mounted: one behind and at the top of the barrier section immediately downstream of the impact which was shown in the simulation to experience the maximum load and displacement, and one on the end of the 1.22 m wide moment slab to monitor the behavior of the moment slab (Figure 13(b)).

Displacement and rotation of the barrier and wall panels were determined from high-speed camera operating at 1000 frames/second. Displacement gages were placed at the top and bottom of the precast barrier-coping section and on the wall panels at heights corresponding to the three layers of soil reinforcement.

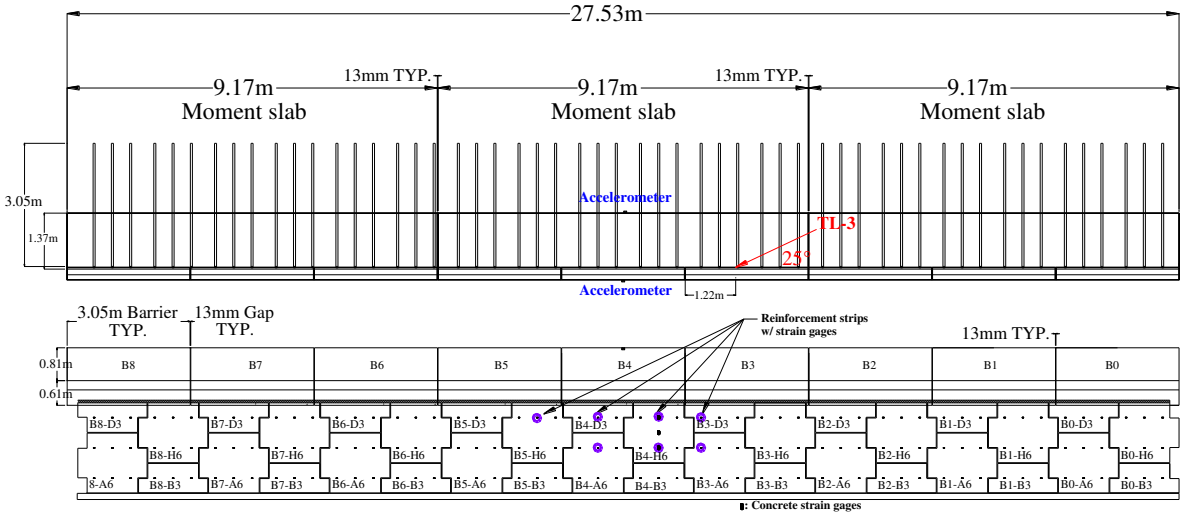

a)

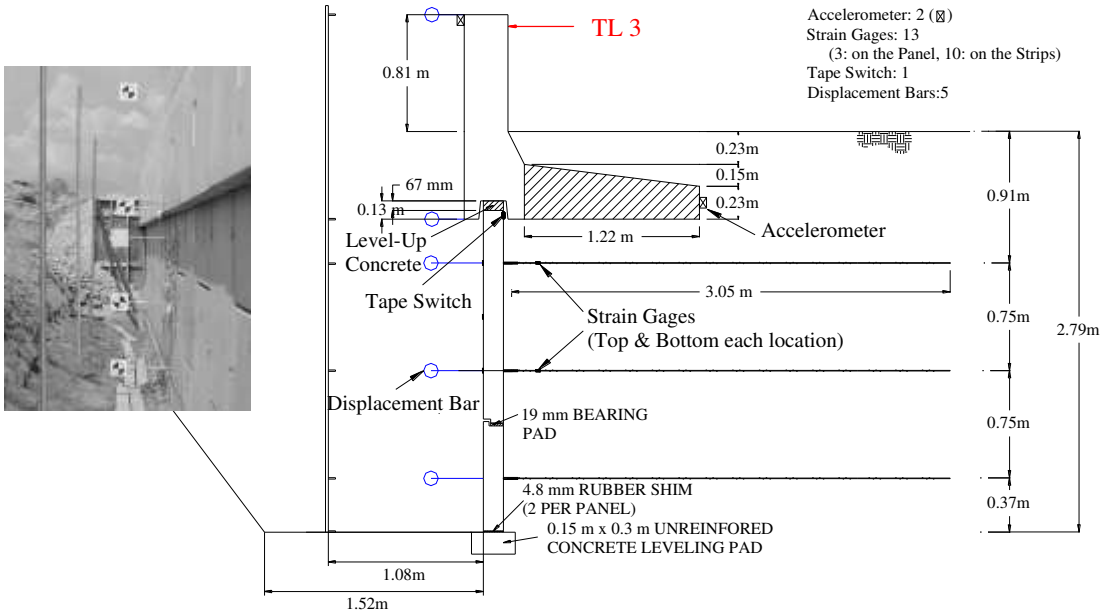

b)

Figure 13: Drawing of barriers on MSE wall: (a) top and plan view and (b) side view (Kim et al. 2012)

7.3 Test Description and Impact Test Results

The TL-3 crash test guidelines described in the Manual for Assessing Safety Hardware (MASH 2009) were followed. This MASH test calls for a 2270P vehicle weighing 2270 kg hitting the barrier at a speed of 100 km/h at an angle of 25 degrees.

The 2004 Dodge Ram 1500 quad-cab pickup truck (Figure 14) used in the test weighed 2246 kg and was instrumented with three solid-state angular rate transducers to measure roll, pitch, and yaw rates; a triaxial accelerometer near the vehicle center of gravity (C.G.) to measure longitudinal, lateral, and vertical deceleration levels; and a backup biaxial accelerometer in the rear of the vehicle to measure longitudinal and lateral deceleration levels.

7.3.1 Dynamic impact load and displacement results

The 2270P vehicle impacted the MSE wall at a velocity of 101.7 km/h and 25.6 degrees. The location of the impact point was 1.22 m upstream of the fourth barrier joint (Figure 13). Figure 14 shows the sequential photos for crash test. The maximum 50 msec. average longitudinal and lateral accelerations were -6.5 g and 15.67 g, respectively. Data obtained from the truck-mounted accelerometer were analyzed to estimate the impact force using eq. (15).

$$F_i(t) = F_x(t)\sin\beta(t) - F_y(t)\cos\beta(t) = m\left(\vec{a}_x(t)\sin\beta(t) - \vec{a}_y(t)\cos\beta(t)\right) \quad (15)$$

where $F_i(t)$ is the impact force; $\beta(t)$ is the vehicular impact angle as a function of time (yaw angle); $F_x(t) = m\vec{a}_x(t)$ is the longitudinal component of the inertia force; $F_y(t) = m\vec{a}_y(t)$ is the lateral component of the inertia force; and m is the mass of the truck.

The maximum 50 msec. average resultant impact force was 371.3 kN at a time of 0.062 sec. as shown in Figure 15(a). Eq. (15) assumes that the vehicle is a rigid body. In fact, crushing of the front end takes place during the impact. This crushing process absorbs energy and therefore the force obtained from eq. (15), 371.3 kN will be higher than the real force. The numerical simulations of this full scale tests indicated that the real force was 248 kN. According to those numbers the impact force is 67% of the force calculated by eq. (15) (Kim et al. 2012).

Figure 14: Sequential photos of MASH test 3-11 **(***Kim et al. 2012).*

The displacement was measured in two ways: videotaping of targets affixed to the wall and barrier, and measurements of permanent displacement after the impact with respect to a benchmark away from the test area. Ten millimeter diameter 0.3 m long steel bars were secured to the top and bottom of the barrier as well as to the top and bottom of the first panel at the level of the strip locations. Targets were attached to the steel bars and were monitored during the impact by a high-speed camera (Figure 13(b)). Note that the location of the targets corresponds to the centerline of panel (B5-H6). The initial position on the movie before impact provided the initial position of the targets and the displacements were recorded with reference to that initial position. Two distinct impacts are evident in the displacement data corresponding to the front end and rear end of the vehicle during the impact. The dynamic displacement associated with the initial impact of the barrier was 21.3 mm at the top of the barrier and 13 mm at the bottom of the barrier (coping) as shown in Figure 15(b). After the first impact, the barrier began to rebound. The subsequent rear end impact (back slap) resulted in dynamic

displacements at the top of the barrier and bottom of the coping of 18.8 mm and 14 mm, respectively. Therefore the first impact was more severe than the back slap impact. The permanent displacement of the barrier was 9.4 mm at the top of the barrier and 6.4 mm at the bottom of the coping. The maximum dynamic displacement of the panel was 10.7 mm at the level of the upper most layer of reinforcement while the permanent displacement was 6.1 mm at the same location. No movement was measured at the level of the second reinforcement layer.

After the impact and when the vehicle had come to rest, the permanent deflection measured with respect to the benchmark ranged from 13 mm at the top of the joint between barrier segment “B4” and “B5” to 1 mm at the bottom of the coping on barrier segment “B5” (Figure 13(a)). The permanent deflection obtained from the film analysis, which tracked the targets placed at the end of the displacement bars affixed to the barrier-coping section, was 9.4 mm at top of the barrier and 6.4 mm at the bottom of the coping. All the displacement measurements indicated that the wall and barrier movement are within the tolerance of 25 mm; therefore the wall and the barrier were satisfactorily designed.

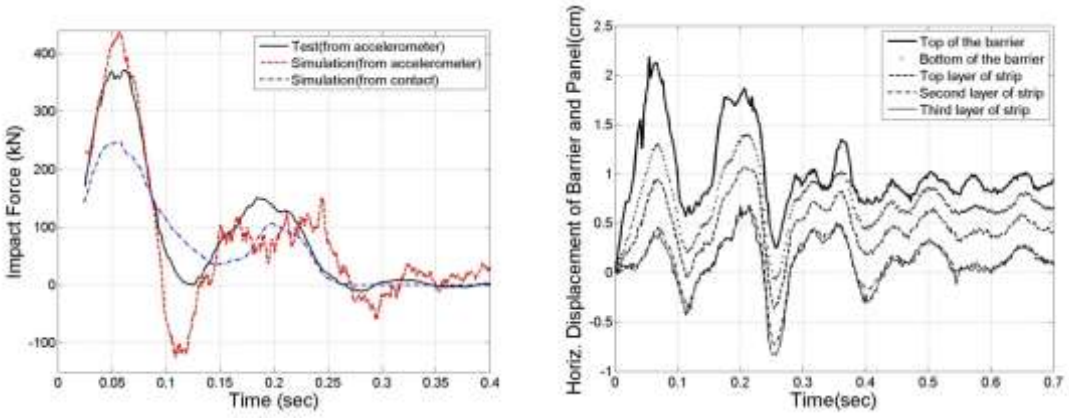

a) *b)*

Figure 15: a) Impact load, b) displacement results (Kim et al. 2012).

7.3.2 Loads in the wall reinforcement

To enable comparison of forces and displacements, barriers and selected strip locations were assigned alphanumeric designators that describe their horizontal position and vertical reinforcement layer. For example, strip “B4-B-1st” is the strip on barrier B4 at position B and in the first (i.e., upper) layer of reinforcement as shown in Figure 16(a).

The static pull out resistance of the strips was calculated according to AASHTO LRFD and is shown in Table 5. The static load in the strips due to the earth pressures behind the wall was measured during the construction of the wall. The strain gages on the strips were re-zeroed before the impact test. The dynamic loads generated during the impact test were measured and are shown in Figure 16(b) as 50 msec. averages as a function of time. The maximum value of the raw data and 50 msec. averages are shown in Table 6. Note that all those measured values correspond to a maximum load of 371.3 kN obtained as the truck mass times the maximum truck deceleration. This load is larger than the maximum impact force at the truck-barrier point of impact because it ignores the strain energy absorbed by the crushing of the truck body. The true impact force was estimated from the numerical simulation as 248 kN which is reasonably close to the barrier dynamic design load of 240 kN prescribed by AASHTO LRFD.

As can be seen from Table 5 and Table 6, the total load measured in the first level of reinforcement exceeds the calculated pull out resistance by AASHTO significantly. Since the measured load was about two times larger than the AASHTO calculated load, and since the panel pulled out about 10 mm during impact, it is possible that the strips were at pull out failure during the impact. Indeed a pull out movement of 10 mm is typically sufficient to generate the full friction of a soil steel interface for a relatively rigid member such as a strip. It is also possible that the calculated pull out resistance was underestimated by the use of lower bound values of F^* for the friction between the strips and the soil as recommended by AASHTO LRFD. It is also possible that the dynamic resistance is higher than the static resistance; however this possibility was dispelled by tests performed at different rates in an

earlier part of the study (Kim et al. 2012). In any case, even if the strips were at pull out failure during the impact as allowed in the proposed guidelines, the wall behaved very satisfactorily and it would be fine to have the strips at pull out failure for this extreme and very short duration event. A more proper design would consider a deflection based design as is done in earthquake engineering (Wartman et al. 2006); this approach is more complicated but more fundamentally acceptable and work is progressing in that direction.

Table 5: Measured loads and calculated resistances for the wall reinforcement (Kim et al. 2012).

	Static Load (measured) (kN)	Dynamic Load [a] (measured) (kN)	Measured Total Loads (kN)	Calculated Unfactored Ultimate Resistance[b] (kN)
Top Layer	3.34	9.79	13.12	6.41
Second Layer	8.23	2.94	11.16	12.01

[a] This dynamic load is the maximum of the max. 50-msec average loads in Table 2.
[b] AASHTO LRFD Eq. 11.10.6.3.2-1

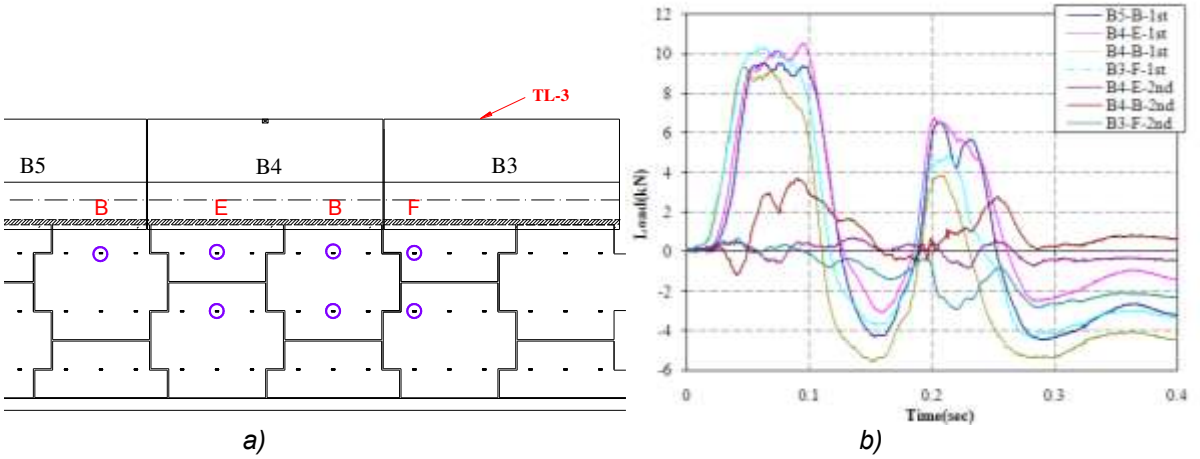

Figure 16: Location indicators and dynamic strip load. (Kim et al. 2012)

Table 6: Measured dynamic loads in excess of the static loads in the wall reinforcement during impact (Kim et al. 2012)

	Top layer (kN)			
	B5-B-1st	B4-E-1st	B4-B-1st	B3-F-1st
Maximum Load from Raw Data	9.56	10.54	9.34	10.32
Maximum 50-msec avg. Load	9.25	9.83	8.63	9.79
	Second Layer (kN)			
		B4-E-2nd	B4-B-2nd	B3-F-2nd
Maximum Load from Raw Data		0.71	3.69	0.67
Maximum 50-msec avg. Load		0.40	2.94	0.27

7.3.3 Damage to the barrier and wall panels

The panels did not crack during the impact. This was later confirmed by observation. The contact switch placed on the top edge of the level-up concrete on top of the wall panel inside the coping recess indicated that the coping did not contact the wall panel. Damage to the barrier was mostly cosmetic. There was a crack in the soil along the edge of the moment slab. This crack was about 2 mm wide and existed over two moment slabs, from B0 to B5, for a length of 18 m (Figure 13(a)).

Overall the test was deemed successful because the vehicle did not go over the barrier, did not roll over, and was safely redirected on the road way.

9. SUMMARY AND CONCLUSIONS

Guidelines for traffic barriers on top of MSE walls were developed on the basis of full scale bogie and pickup truck tests (Bligh et al. 2009; Briaud et al. 2009; Kim et al. 2012) and are presented in an LRFD format. They address pullout and rupture of the MSE wall reinforcement, structural adequacy of the MSE wall panels, sliding and overturning of the barrier-moment slab system, and structural adequacy of the coping. The dynamic design loads for the reinforcement are specified using a pressure distribution approach or a line load approach.

A full-scale pickup truck (TL-3) crash test into a vertical wall barrier mounted on the edge of a 2.78 m tall MSE wall was performed. Damage and displacement of the MSE wall panels and the barrier system were minimal and within tolerance. The load in the top level of reinforcement was much higher than the maximum load calculated by AASHTO-LRFD Bridge Specifications. This is due to the fact that these specifications are quite conservative. These high loads also mean that the reinforcement could have been at pull out failure during most of the impact. This situation is deemed acceptable and allowed in the guidelines because it occurs over a very short period of time (about 20 ms) and because the observed wall displacement during that very short time is within tolerance (less than 25 mm). A more proper design would consider a deflection based design; this approach is more complicated but more fundamentally acceptable and work is progressing in that direction.

The barrier was made of 3.05 m long precast barrier-coping sections connected to a 1.37 m wide and 9.17 m long moment slabs and performed as well as the wall. This wall barrier system was designed according to the guidelines presented at the beginning of the paper. It behaved very well and no repairs would be necessary. Since it performed very well, this full scale crash tests represents a verification of the proposed guidelines.

10. ACKNOWLEDGMENTS

The content of this paper presents a summary of the final result of a project sponsored by the National Cooperative Highway Research Program (NCHRP). The opinions expressed in the paper are those of the authors and not necessarily those of NCHRP. The authors wish to thank the research team involve in that project, Dr. Roger Bligh, Dr. Akram Abu-Odeh and Dr. Kang-mi Kim, and the NCHRP panel members for their input and help in particular Mark McClelland, chair of the panel. The authors also wish to sincerely thank the Reinforced Earth Company (Pete Anderson, John Sankey) for providing the barrier, sharing data, and answering many questions. Finally, the authors wish to thank Foster Geotechnical (William Neely) for sharing their experience on MSE walls.

REFERENCES

AASHTO. (2004). *AASHTO LRFD bridge design specifications*, 3rd Ed. AASHTO, Washington, D.C.

AASHTO. (2007). *AASHTO LRFD bridge design specifications*, 4rth Ed. AASHTO, Washington, D.C.

AASHTO. (2009). Manual for Assessing Safety Hardware, AASHTO, Washington, D.C.

Beason, W.L. and T.J. Hirsch (1989). Measurement of heavy vehicle impact forces and inertia properties. Research Report, Texas Transportation Institute, College Station, TX, 1989.

Bligh, R. P., Briaud, J.-L., Abu-Odeh, A. Kim, K.-M and Saez, D.-O. (2011). “Interim Report: Design Guidelines for TL-3 through TL-5 roadside barrier systems placed on mechanically stabilized earth (mse) retaining walls”, *Interim report prepared for National Cooperative Highway Research Program project 22-20(2)*, Transportation Research Board, National Research Council, performed by Texas Transportation Institute, College Station, Tex.

Bligh, R. P., Briaud, J.-L., Kim, K.-M. and Abu-Odeh, A. (2009). “Design of roadside barrier systems placed on mse retaining walls”, *Final report prepared for National Cooperative Highway Research Program project 22-20*, Transportation Research Board, National Research Council, performed by Texas Transportation Institute, College Station, Tex.

Briaud, J.-L., Bligh, R. P., Abu-Odeh, A., and Kim, K. (2008). “Stability analysis and full scale test of a traffic barrier-moment slab system”, *Transportation Research Record: Journal of the Transportation Research Board*, Volume 2050, 26-38.

Kim, K-M. Briaud, J.-L., Bligh, R. P., Abu-Odeh, A., and Saez D. O. (2012). “Design Guidelines and full scale verification for MSE wall with traffic barriers”*, Journal of Geotechnical and Geoenvironmental Engineering*, Vol. 137, No.6, ASCE.

Kim, K-M. Briaud, J.-L., Bligh, R. P., and Abu-Odeh, A. (2010). “Full scale impact testing of four traffic barriers on top of an instrumented MSE wall”*, Journal of Geotechnical and Geoenvironmental Engineering*, Vol. 136, No.3., ASCE.

LS-DYNA: Keyword User's Manual, Version 971, Livermore Software Technology Corporation, Livermore, California, 2007.

Ross, H.E., Jr., D. L. Sicking, R. A. Zimmer, and J. D. Michie (1993). *NCHRP Report 350: Recommended Procedures for the Safety Performance Evaluation of Highway Features*. Transportation Research Board of the National Academies, Washington, D.C., 1993

Texas Department of Transportation (2004). Standard specification for construction and maintenance of highways, streets, and bridges. TxDOT, June 2004.

Wartman, J., Rondinel-Oviedo, E. A., Rodriguez-Marek, A. M. (2006). “Performance and Analysis of Mechanically Stabilized Earth (MSE) Walls in the Tecomán, Mexico Earthquake,” *Journal of Performance of Constructed Facilities*, Vol. 20, No. 3, pp. 287-299.